

# Relation between Local Structure, Electric Dipole, and Charge Carrier Dynamics in DHICA Melanin: A Model for Biocompatible Semiconductors

Micaela Matta,\* Alessandro Pezzella, and Alessandro Troisi

Cite This: *J. Phys. Chem. Lett.* 2020, 11, 1045–1051

Read Online

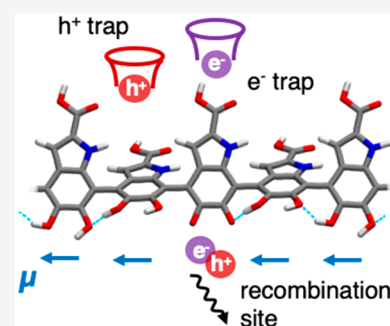
ACCESS |

Metrics & More

Article Recommendations

Supporting Information

**ABSTRACT:** Eumelanins are a family of natural and synthetic pigments obtained by oxidative polymerization of their natural precursors: 5,6-dihydroxyindole and its 2-carboxy derivative (DHICA). The simultaneous presence of ionic and electronic charge carriers makes these pigments promising materials for applications in bioelectronics. In this computational study we build a structural model of DHICA melanin considering the interplay between its many degrees of freedom, and then we examine the electronic structure of representative oligomers. We find that a nonvanishing dipole along the polymer chain sets this system apart from conventional polymer semiconductors, determining its electronic structure, reactivity toward oxidation and localization of the charge carriers. Our work sheds light on previously unnoticed features of DHICA melanin that not only fit well with its radical scavenging and photoprotective properties but also open new perspectives toward understanding and tuning charge transport in this class of materials.



Melanins are a family of natural pigments ubiquitous in mammals and invertebrates. Among them, eumelanin is the dark pigment present not only in human skin and hair but also in eyes and nigral neurons.<sup>1</sup> Due to its dual protonic and electronic conductivity<sup>2–4</sup> and intrinsic biocompatibility, eumelanin is currently being investigated as an active material in supercapacitors for energy storage,<sup>5,6</sup> organic electrochemical field effect transistors (OECTs) for sensing or diagnostics devices, such as cells/nerves stimulation and signal amplification.<sup>7–12</sup> Natural eumelanin consists of amorphous aggregates obtained by oxidative polymerization of 5,6-dihydroxyindole (DHI) and its 2-carboxylic acid derivative (DHICA), interacting via  $\pi$ -stacking and hydrogen bonding (see Figure 1a). DHI exhibits self-coupling at positions 2, 4, and 7; in DHICA, only positions 4 and 7 are reactive. The structural ambiguity of natural eumelanin, which contains both DHI and DHICA, is partly due to the range of possible binding motifs between the two building blocks and results in a lack of long-range structural order.<sup>13,14</sup> The development of synthetic DHICA and DHI melanins<sup>15</sup> has paved the way toward a more systematic understanding of the structural, redox, optical, and aggregation-dependent properties of eumelanin. The lower chemical disorder and better reproducibility make these polymers ideal candidates for exploring the potential of eumelanin in bioelectronic applications, either by itself or as a component in hybrid scaffolds.<sup>16</sup>

However, despite its promising characteristics, eumelanin-based devices are still in their infancy. The lack of consensus regarding the molecular structure of both natural and synthetic eumelanin has prevented the rational optimization of semi-

conducting interfaces based on this biopigment. Moreover, several controversies regarding key properties of eumelanin are yet to be definitively settled. The relative importance of ionic and electronic charge carriers, the influence of water on conductivity, and the activity of radical species are still the subject of intense academic debate.<sup>17</sup> Several studies argue that the observed increase in conductivity of eumelanin is hydration dependent and therefore identify the primary charge carriers as protons.<sup>18</sup> However, other studies point at evidence of both electronic and protonic charge transport,<sup>4</sup> and a more recent work reports the highest conductivity ever recorded in vacuum-annealed (anhydrous) eumelanin films.<sup>2</sup>

Modeling and simulations are therefore indispensable to tackle these issues and push the boundaries of eumelanin bioelectronics. Previous theoretical investigations have focused on reproducing the photophysical features of eumelanin by studying binding motifs between monomers, and  $\pi$ -stacking of small oligomers.<sup>19–21</sup> Other studies have employed molecular dynamics to reproduce the short-range ordered structure of eumelanin amorphous aggregates, focusing on porphyrin-like tetramers.<sup>22</sup> Overall, the vast majority of literature has concentrated mostly on planar oligomers of DHI, while DHICA melanin has only been studied marginally.<sup>23,24</sup>

Received: December 13, 2019

Accepted: January 22, 2020

Published: January 22, 2020

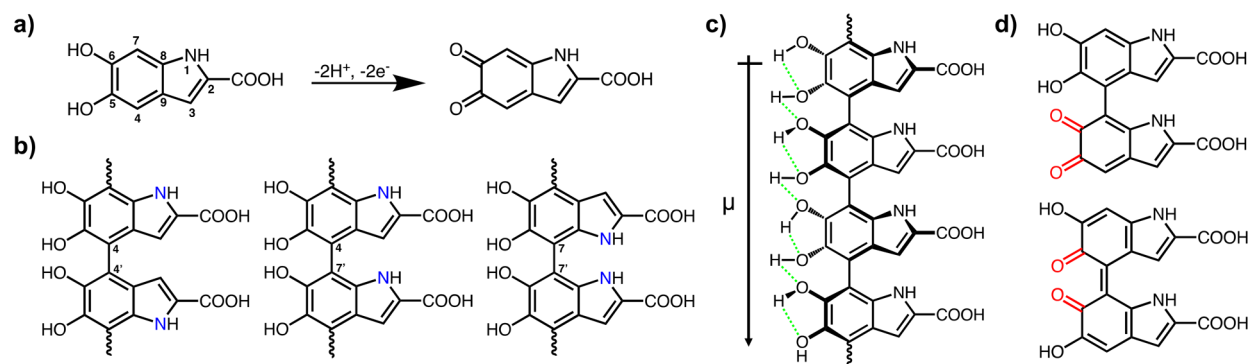


**Figure 1.** (a) Molecular structure and ring numbering of DHICA in the reduced indole (left) form and in the oxidized quinone form (right). (b) Different tacticity in DHICA melanin originating from 4,4' (left), 4,7' (center), and 7,7' (right) bonds. Rotation around these single bonds is sterically hindered. (c) Scheme of a DHICA tetramer highlighting the atropoisomerism, the hydrogen bonds network and the direction of the oligomer dipole. (d) Localized (top) and distributed (bottom) oxidation pattern for quinones.

Remarkably, no studies have so far investigated charge transport on either system.

The charge transport mechanism of eumelanin is undoubtedly the area where a theoretical insight is most needed to integrate state of the art experimental observations. If we treat eumelanin as a member of the general class of polymer semiconductors, we can assume electron or hole transport would involve the study of more or less extended charge carrier states, which are in turn determined by the local microstructure of the material, its mesoscopic properties, and its relative disorder.<sup>25,26</sup> However, eumelanin differs from the typical semiconducting polymer in several nontrivial ways, which characterize its structural disorder. For instance, the hydroxyl units are responsible for the presence of multiple oxidation states; its hydrogen bonds create a nonvanishing dipole across the polymer chain, and the nonsymmetric nature of its monomers makes the corresponding polymers not regioregular.

In the specific case of DHICA melanin, we have categorized the degrees of freedom that can be seen as the origin of the structural disorder in the polymer:

**Tacticity/Regiochemistry.** For both DHI and DHICA, position 4 and 7 are not equivalent, giving rise to different binding motifs illustrated in Figure 1b and denoted as 4,4', 7,7' and 4,7'. Oligomers with different regiochemistry have been isolated,<sup>23,27</sup> but the distribution of tacticity in realistic materials and its effect on the electronic structure are not known.

**Conformational Isomerism (Atropoisomerism) and Helicity.** The rotation around the C–C' bonds is hindered; thus different diastereoisomers are possible for the same chemical connectivity, depending on the dihedral angles between indole units. Helicity, defined as the collective orientation of all dihedrals between monomers, not only influences the DHICA polymer shape but also could affect interchain interactions and aggregation.

**Hydrogen Bond Network.** Nonbonded interactions, particularly inter- and intrachain hydrogen bonds and interchain  $\pi$ -stacking, might strongly affect the polymer structure. In particular the –OH groups form a 1D chain of H-bond donor/acceptor (see Figure 1c) which can, in principle, dictate the local conformation of the polymer.<sup>24</sup>

**Oxidation State and Redox Disorder.** DHICA oligomers tend to oxidize as the polymer grows beyond  $\sim 10$  repeating units,<sup>28</sup> the main oxidized species being the quinone. The distribution

of quinone units within the polymer is not completely understood, but it is estimated that one in 20 monomers is oxidized.<sup>29,30</sup> Two main oxidation patterns are possible: distributed and localized (see Figure 1d), with the latter being more stable according to prior studies. The presence of oxidized groups gives DHICA melanin its spectroscopic signature, being responsible for the broad absorption in the UV–vis region. The change in electronic structure upon oxidation is bound to affect the charge transport properties, although this aspect has not been investigated so far.

In this work, we study DHICA oligomers to establish how the many degrees of freedom of this system interact to determine the most stable structure, working our way from the highest interconversion barriers to the lowest: tacticity, atropoisomerism, helicity, hydrogen bond network. Once the hierarchy of structural degrees of freedom is established, we turn our attention to oxidized oligomers and the effects of oxidation on the electronic structure of this polymer, concluding with general considerations about the most likely charge transport mechanisms in bulk, anhydrous DHICA melanin. Note that we have intentionally left aside intermolecular interactions and aggregation effects. While these might affect excited state properties and redox equilibria of solvated DHICA melanin,<sup>31</sup> they are unlikely to alter the structure, ground state properties, and possibly the electronic transport mechanism in the bulk anhydrous polymer. In fact, unlike DHI-containing melanins, DHICA melanin forms amorphous, loosely bundled aggregates where  $\pi$ -stacking is expected to be marginal.<sup>32,33</sup> Our modeling strategy has been informed by the available experimental data outlined above.

**Tacticity and Conformational Isomerism.** Neutral DHICA dimers were initially optimized at the  $\omega$ B97X-D/cc-pVTZ level. After verifying that the basis set size has a very marginal effect on relative energies and dipole moments (see Supporting Information, Table S2), all calculations on larger systems were performed using the more cost-effective basis set 6-31G\*. Note that only  $\sim 1\%$  of the carboxylic groups in DHICA are expected to be deprotonated in water, and we are interested specifically in the behavior of the dry polymer; therefore, we focused on neutral oligomers. As previously reported, all 4,4', 4,7', and 7,7' DHICA dimers have their lowest energy minimum at  $\sim 50^\circ$  (see Supporting Information, Figure S1), characterized by an intermonomer hydrogen bond. The 4,7' isomer is the most stable, followed by 4,4' and 7,7' (higher in energy by 0.84 and 1.68 kcal/mol, respectively). Even when environmental

dielectric effects are included, the 4,7' dimer remains the most stable species, while the difference in relative energy between 4,4' and 7,7' is reduced to 0.07 kcal/mol (see Supporting Information, Table S2). Regardless of energy differences, all three minima look similar and the curvature of their potential energy surface is almost identical. Remarkably, the three most stable dimers have very similar dipole moments (5.5–5.8 D, the highest being for the 4,7' dimer), oriented along the polymer growth axis and largely due to the inter- and intramolecular hydrogen bonds. These findings highlight the limited importance of tacticity in the conformational landscape of DHICA melanin and, we argue, in determining its charge transport properties. Therefore, for the remainder of this discussion we will focus on 4,7' regioregular oligomers.

**Helicity and Hydrogen Bond Network.** We considered two hypotheses regarding the collective orientation of dihedrals in longer oligomers: they can be arranged in a zigzag fashion, alternating  $\pm 50^\circ$  dihedrals, or in a helix shape, all dihedrals having the same sign, as shown in Figure 2a. The zigzag shaped oligomers are only slightly preferred to the helix shaped, by 0.28 (0.87) kcal/mol for tetramers (octamers). As the difference between the two conformations is substantially smaller than typical intramolecular interactions (i.e., hydrogen bonds), we can assume the final helicity (defined as the sequence of dihedrals between monomers) will be likely determined by the local environment, which lies outside the scope of this study.

Both zigzag and helix oligomers are stabilized by an uninterrupted chain of hydrogen bonds in the same direction of the indole dipole, with hydroxyl groups pointing the opposite way with respect to the nitrogen (see Figure 2a). The consequence of the hydrogen bond directionality is that the individual dipoles of each monomer (2.9 D) are summed to give a strong, permanent dipole in both helix and zigzag conformations. (Figure 2b). The energy penalty to reverse the direction of all hydrogen bonds is 2.97 (3.02) kcal/mol for a zigzag (helix) tetramer. We also investigated the penalty for the disruption of the hydrogen bond and dipole continuity by flipping half of the C–C–O–H dihedrals in the opposite direction for tetramers. The energy penalty was found to be 10.3 (9.96) kcal/mol for the zigzag (helix) conformation, and rather insensitive to the chain length (see Figure S1 and Table S4). Interestingly, the energy difference between the zigzag and helix conformations is reduced to just 0.06 kcal/mol once the chain of hydrogen bonds is disrupted (Figure S2 and Table S4). These observations denote that hydrogen bonds and torsional energies are additive.

In summary, tacticity and helicity are predicted to have little effect on the electronic structure of DHICA melanin; the most stable arrangement of dihedrals maximizes the internal dipole by forming an uninterrupted chain of hydrogen bonds. However, we must point out that the energy cost to disrupt the dipoles could be easily circumvented via the formation of intermolecular hydrogen bonds; we are not considering this possibility, which will be explored in our future work.

**Oxidation to Quinone.** Once the hierarchy of interactions dictating the conformational space of DHICA oligomers was established, we studied the corresponding quinones, under the generally accepted assumption that polymerization (at least in its initial phase) happens prior to oxidation.<sup>28</sup> Helix and zigzag tetramers were oxidized to quinones; all possible oxidation patterns, both distributed and localized, were explored (see Supporting Information, Figure S3). As expected, localized

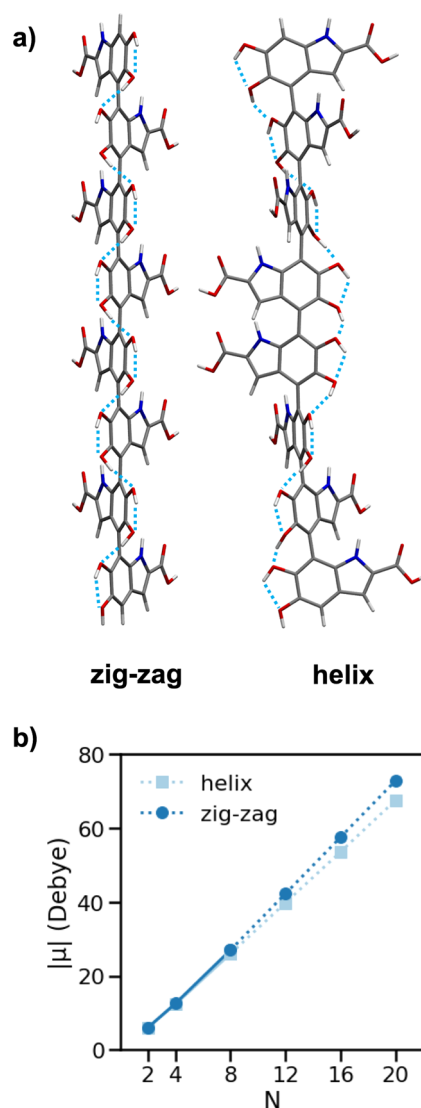


**Figure 2.** (a) Optimized geometries of octamers in the zigzag and helix conformations, with dotted lines highlighting the chain of hydrogen bonds. (b) Absolute magnitude of the dipole as a function of oligomer length  $N$  for a series of zigzag and helix oligomers. Points connected by solid lines indicate fully optimized geometries at  $\omega$ B97X-D/6-31G\* level, dashed lines identify  $\omega$ B97X-D/6-31G\* single-point calculations on longer oligomers obtained by rigid translation of shorter segments.

quinones are energetically preferred by 1.4 (0.9) kcal/mol for zigzag (helix) tetramers. Interestingly, there is a strong effect of the internal dipole, which favors oxidation on the terminal (negative) monomer, followed by the second to last (0.3 kcal/mol higher in energy), and makes the opposite (positive) end harder to oxidize (3.75 and 4.53 kcal/mol more endothermic for zigzag and helix tetramers, respectively). As seen for the corresponding indoles, the energy difference between the two most stable quinones in either zigzag or helix conformation remains rather small at 0.43 kcal/mol. Since chain helicity does not seem to affect the relative stability of quinone isomers, we will only focus on longer oligomers in the zigzag conformation.

We then studied the interaction between quinones by oxidizing two monomers on the same zigzag octamer. Using the most stable singly oxidized species as references, we calculated the energy penalty for the products of a second

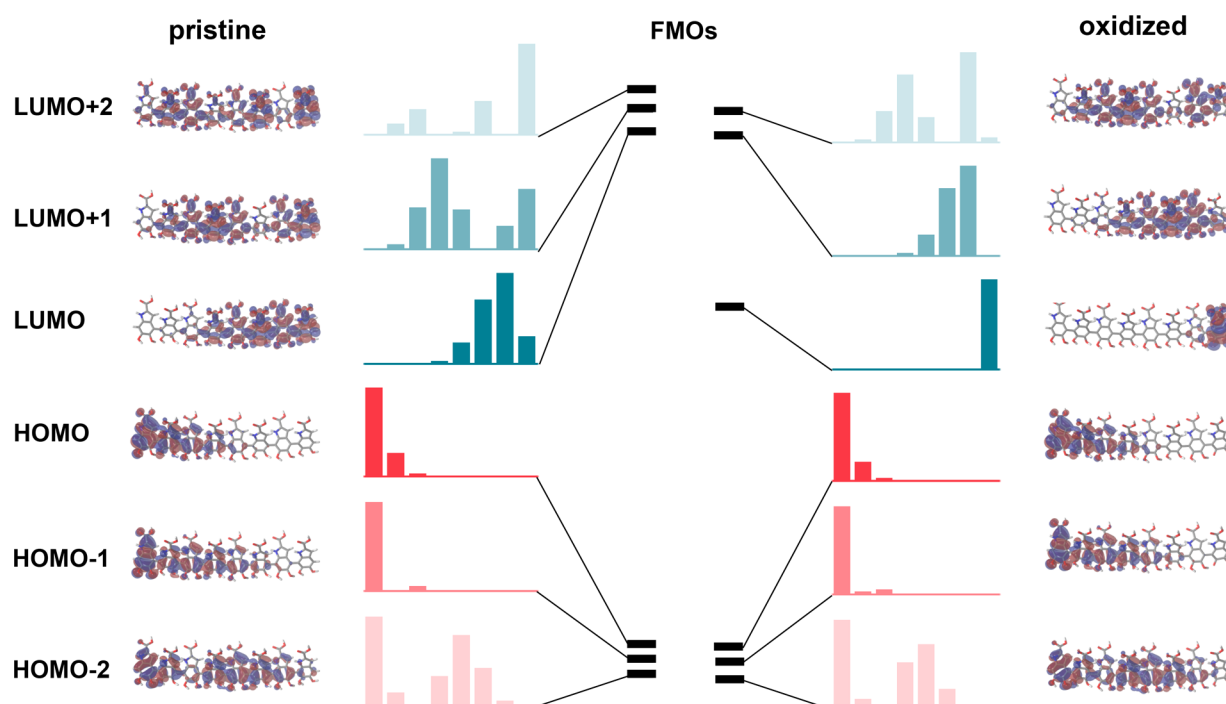


**Figure 3.** Frontier molecular orbitals (HOMO–2 to LUMO+2), squared fragment orbital population coefficients on each monomer obtained from the Mulliken population analysis, and energy diagram of the reduced (left) and oxidized (right) octamers.

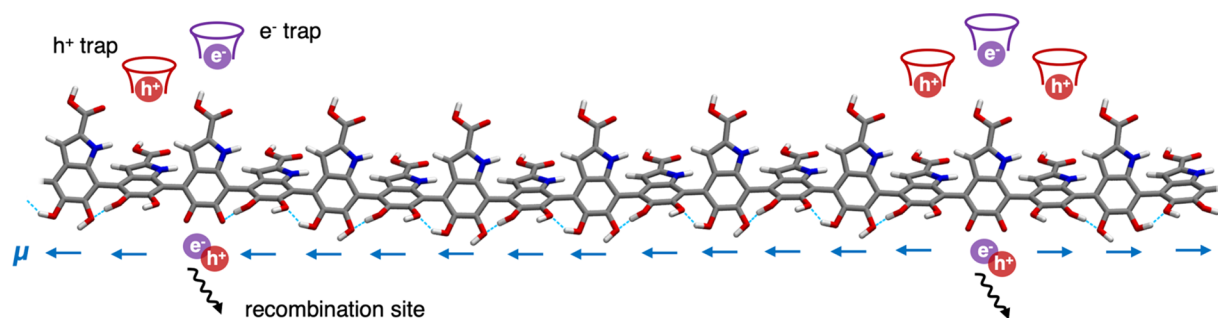


**Figure 4.** Scheme of a DHICA melanin segment showing typical recombination and trapping sites for holes and electrons. The monomer dipoles (blue arrows) follow the direction of the hydrogen bonds.

oxidation at different positions with respect to the first quinone (see Supporting Information, Figures S4 and S5a). The results show that a second oxidation is less energetically favored near an already oxidized indole suggesting that the oxidation sites have a tendency to be segregated. In general, we would expect oxidation to occur at a position that minimizes the repulsion with other quinones and maximizes the distance from the positive end of the dipole. Quinone units introduce a discontinuity in the hydrogen bond network, so DHICA melanin can be visualized as made of long segments with unidirectional hydrogen bonds interrupted by oxidized units. We must finally point out that our results are independent of the specific density of oxidized indoles being used as long as these represent a small minority.<sup>31</sup>

**Energy Landscape and Transport Mechanism of Oxidized Oligomers.** We analyzed the changes in the electronic energy states of oxidized oligomers with respect to their reduced analogues, in particular the shape and localization of frontier molecular orbitals (FMOs). In both species, the strong permanent dipole affects the shape of the frontier orbitals: while the HOMO is localized toward the negatively charged

side of the oligomer, the situation is reversed for the LUMO (see Figure 3, left side). This striking effect, unseen in canonic semiconducting polymers, does not stem from the nature of the  $\pi$ -conjugated system but rather from polar functional groups not involved in conjugation. Oxidation is accompanied by the appearance of a low lying LUMO localized on the quinone unit, leaving the other FMOs unperturbed (see the right-hand side of Figure 3). Regardless of the oxidation position, to each quinone corresponds a localized state adding to the lowest energy band in the polymer (Supporting Information, Figure S4b).

The electronic properties of representative DHICA oligomers allow us to formulate predictions on the charge carrier behavior in DHICA melanin. As far as holes are concerned, the internal dipole of the polymer affects the shape and localization of the HOMO and constitutes a new type of long-range, correlated disorder contributing to the localization of holes. As seen in Figure S2, the position of the HOMO along the DHICA oligomer is strongly affected by the dipole orientation; this would seem to favor the localization of holes and electrons in different segments, at least in small oligomers

with only one oxidation defect. However, a more representative model oligomer would be a longer segment where a series of indole units are delimited by a quinone on either end (see Figure 4). In this model system, regardless of the local dipole orientation, the hole is found to overlap with one of the two quinone-centered monomers. The energy to escape this local trap, either toward another localized state<sup>34</sup> or to a more delocalized state, is given by the reorganization energy,  $\lambda_+ = \sim 0.8$  eV (see Supporting Information, Table S5). The density of these traps is comparable to the density of oxidized units and typically similar or larger to the carrier density achievable in transistor devices, we expect these localized states to determine the carrier mobility in most conditions. This is a highly unusual scenario for polymer semiconductors, where conformational disorder is the main factor affecting charge transport.<sup>35–37</sup>

Conversely, electrons are expected to be localized on isolated oxidized monomers, the electron affinity of an oxidized oligomer being 2.3 eV higher than that of its polyindole analogue (see Table S5). Given the low density of quinones across the polymer chain, as well as the significant energy difference between these trap states and the higher, more delocalized unoccupied states, we do not anticipate electron transport to be relevant in DHICA melanin.

Interestingly, the ambiguity surrounding the exact nature of the spatially confined and roughly homogeneous free radical species in DHICA melanin,<sup>32</sup> characterized by a narrow EPR signal, seems to be in agreement with our findings regarding the spatial localization of both holes and electrons.

As for the fate of electron–hole pairs, the significant spatial overlap between localized holes and electrons is expected to lead to efficient charge recombination. This would be the case when electron–hole pairs are photochemically generated, thus agreeing with the efficient nonradiative energy dissipation mechanism crucial for the pigment's photoprotective activity.<sup>33</sup>

In this work, we uncovered a number of features that set DHICA melanin aside from other biopolymers as well as common organic semiconductors. We set out to study the regiochemistry and conformational freedom of DHICA melanin, only to discover their marginal role in determining both the charge carrier and orbital localization. The electronic structure of DHICA melanin is surprisingly and substantially affected by its strong dipole moment, which localizes frontier orbitals on small molecular segments and impacts the polymer charge transport mechanism. The formation of one-dimensional chains of hydrogen bonds is DHICA melanin's defining structural feature, and their orientation directly affects the dipole magnitude. The disruption of the hydrogen bond network due to intermolecular interactions is anticipated to be one of the main sources of electronic disorder in the bulk, which, however, does not affect the validity of our findings. Oxidation is instead shown to create extremely localized virtual orbitals, building up a separate band in the density of states of the bulk polymer. Hole transport in DHICA melanin is likely to happen via hopping, however, limited by the presence of deep trap states. Future studies aimed at obtaining a full picture of DHICA melanin will take into account the effect of stabilizing interchain interactions, chain flexibility, and a higher dielectric environment that would concur to reduce the hydrogen bond orientational order.

The wider impact of our findings is related to the possible role of eumelanin as a biocompatible semiconductor. To this end, we can anticipate chemical modification and functional-

ization to play a main role in tuning the transport properties in this class of materials, where electrostatic interactions are more important role than nonpolar, van der Waals forces.

## ■ COMPUTATIONAL METHODS

Geometry optimizations were performed with Gaussian16<sup>38</sup> at the  $\omega$ B97X-D/6-31G\* level except where otherwise stated. The Mulliken population analysis was performed using the cclib<sup>39</sup> package.

## ■ ASSOCIATED CONTENT

### Supporting Information

The Supporting Information is available free of charge at <https://pubs.acs.org/doi/10.1021/acs.jpcllett.9b03696>.

Details of conformational searches and electronic structure calculations; tables of optimized parameters, relative energies and dipole moments, orbital energies, ionization potentials, electron affinities, and reorganization energies; figures showing potential energy scans, dipole moments, relative energies and HOMOs, optimized geometries, calculated energy difference and energy level diagrams, and the IP dependence on oligomer length (PDF)

## ■ AUTHOR INFORMATION

### Corresponding Author

Micaela Matta – Department of Chemistry, University of Liverpool, Liverpool L69 7ZD, U.K.; [orcid.org/0000-0002-9852-3154](https://orcid.org/0000-0002-9852-3154); Email: [micaela.matta@liverpool.ac.uk](mailto:micaela.matta@liverpool.ac.uk)

### Authors

Alessandro Pezzella – National Interuniversity Consortium of Materials Science and Technology (INSTM), 50121 Florence, Italy; Composites and Biomaterials (IPCB), Institute for Polymers, I-80078 Pozzuoli, Italy; [orcid.org/0000-0001-6925-922X](https://orcid.org/0000-0001-6925-922X)

Alessandro Troisi – Department of Chemistry, University of Liverpool, Liverpool L69 7ZD, U.K.; [orcid.org/0000-0002-5447-5648](https://orcid.org/0000-0002-5447-5648)

Complete contact information is available at: <https://pubs.acs.org/10.1021/acs.jpcllett.9b03696>

### Author Contributions

M.M. realized the study and wrote the paper. M.M., A.T., and A.P. designed the study.

### Notes

The authors declare no competing financial interest.

## ■ ACKNOWLEDGMENTS

M.M. acknowledges the financial support of the Royal Society in the form of a Newton International Fellowship (NIF \R1\181379).

## ■ REFERENCES

- (1) d'Ischia, M.; Wakamatsu, K.; Cicoira, F.; Di Mauro, E.; Garcia-Borron, J. C.; Commo, S.; Galván, I.; Ghanem, G.; Kenzo, K.; Meredith, P.; et al. Melanins and Melanogenesis: From Pigment Cells to Human Health and Technological Applications. *Pigm. Cell Melanoma Res.* **2015**, *28* (5), 520–544.
- (2) Migliaccio, L.; Manini, P.; Altamura, D.; Giannini, C.; Tassini, P.; Maglione, M. G.; Minarini, C.; Pezzella, A. Evidence of Unprecedented High Electronic Conductivity in Mammalian Pigment

Based Eumelanin Thin Films After Thermal Annealing in Vacuum. *Front. Chem.* **2019**, *7* (March), 1–8.

(3) Wünsche, J.; Cicoira, F.; Graeff, C. F. O.; Santato, C. Eumelanin Thin Films: Solution-Processing, Growth, and Charge Transport Properties. *J. Mater. Chem. B* **2013**, *1* (31), 3836.

(4) Wünsche, J.; Deng, Y.; Kumar, P.; Di Mauro, E.; Josberger, E.; Sayago, J.; Pezzella, A.; Soavi, F.; Cicoira, F.; Rolandi, M.; et al. Protonic and Electronic Transport in Hydrated Thin Films of the Pigment Eumelanin. *Chem. Mater.* **2015**, *27* (2), 436–442.

(5) Kumar, P.; Di Mauro, E.; Zhang, S.; Pezzella, A.; Soavi, F.; Santato, C.; Cicoira, F. Melanin-Based Flexible Supercapacitors. *J. Mater. Chem. C* **2016**, *4* (40), 9516–9525.

(6) Xu, R.; Gouda, A.; Caso, M. F.; Soavi, F.; Santato, C. Melanin: A Greener Route To Enhance Energy Storage under Solar Light. *ACS Omega* **2019**, *4*, 12244.

(7) Piacenti Da Silva, M.; Fernandes, J. C.; De Figueiredo, N. B.; Congiu, M.; Mulato, M.; De Oliveira Graeff, C. F. Melanin as an Active Layer in Biosensors. *AIP Adv.* **2014**, *4* (3), 037120.

(8) Bonadies, I.; Cimino, F.; Carfagna, C.; Pezzella, A. Eumelanin 3D Architectures: Electrospun PLA Fiber Templating for Mammalian Pigment Microtube Fabrication. *Biomacromolecules* **2015**, *16* (5), 1667–1670.

(9) Pezzella, A.; Barra, M.; Musto, A.; Navarra, A.; Alfè, M.; Manini, P.; Parisi, S.; Cassinese, A.; Criscuolo, V.; D'Ischia, M. Stem Cell-Compatible Eumelanin Biointerface Fabricated by Chemically Controlled Solid State Polymerization. *Mater. Horiz.* **2015**, *2* (2), 212–220.

(10) Rivnay, J.; Inal, S.; Salleo, A.; Owens, R. M.; Berggren, M.; Malliaras, G. G. Organic Electrochemical Transistors. *Nat. Rev. Mater.* **2018**, *3* (2), 17086.

(11) Paulsen, B. D.; Tybrandt, K.; Stavrinidou, E.; Rivnay, J. Organic Mixed Ionic–Electronic Conductors. *Nat. Mater.* **2020**, *19*, 13.

(12) Inal, S.; Malliaras, G. G.; Rivnay, J. Benchmarking Organic Mixed Conductors for Transistors. *Nat. Commun.* **2017**, *8* (1), 1767.

(13) Watt, A. A. R.; Bothma, J. P.; Meredith, P. The Supramolecular Structure of Melanin. *Soft Matter* **2009**, *5* (19), 3754–3760.

(14) Clancy, C. M. R.; Nofsinger, J. B.; Hanks, R. K.; Simon, J. D. Hierarchical Self-Assembly of Eumelanin. *J. Phys. Chem. B* **2000**, *104*, 7871.

(15) D'Ischia, M.; Wakamatsu, K.; Napolitano, A.; Briganti, S.; Garcia-Borron, J. C.; Kovacs, D.; Meredith, P.; Pezzella, A.; Picardo, M.; Sarna, T. Melanins and Melanogenesis: Methods, Standards, Protocols. *Pigm. Cell Melanoma Res.* **2013**, *26*, 616.

(16) Di Capua, R.; Gargiulo, V.; Alfè, M.; De Luca, G. M.; Skála, T.; Mali, G.; Pezzella, A. Eumelanin Graphene-Like Integration: The Impact on Physical Properties and Electrical Conductivity. *Front. Chem.* **2019**, *7* (March), 1–12.

(17) Rienecker, S. B.; Mostert, A. B.; Schenk, G.; Hanson, G. R.; Meredith, P. Heavy Water as a Probe of the Free Radical Nature and Electrical Conductivity of Melanin. *J. Phys. Chem. B* **2015**, *119* (48), 14994–15000.

(18) Sheliakina, M.; Mostert, A. B.; Meredith, P. An All-Solid-State Biocompatible Ion-to-Electron Transducer for Bioelectronics. *Mater. Horiz.* **2018**, *5* (2), 256–263.

(19) Prampolini, G.; Cacelli, I.; Ferretti, A. Intermolecular Interactions in Eumelanins: A Computational Bottom-up Approach. I. Small Building Blocks. *RSC Adv.* **2015**, *5* (48), 38513–38526.

(20) Chen, C. T.; Buehler, M. J. Polydopamine and Eumelanin Models in Various Oxidation States. *Phys. Chem. Chem. Phys.* **2018**, *20* (44), 28135–28143.

(21) Chen, C. T.; Martin-Martinez, F. J.; Jung, G. S.; Buehler, M. J. Polydopamine and Eumelanin Molecular Structures Investigated with Ab Initio Calculations. *Chem. Sci.* **2017**, *8* (2), 1631–1641.

(22) Chen, C.-T.; Chuang, C.; Cao, J.; Ball, V.; Ruch, D.; Buehler, M. J. Excitonic Effects from Geometric Order and Disorder Explain Broadband Optical Absorption in Eumelanin. *Nat. Commun.* **2014**, *5* (May), 3859.

(23) Pezzella, A.; Vogna, D.; Prota, G. Synthesis of Optically Active Tetrameric Melanin Intermediates by Oxidation of the Melanogenic

Precursor 5,6-Dihydroxyindole-2-Carboxylic Acid under Biomimetic Conditions. *Tetrahedron: Asymmetry* **2003**, *14* (9), 1133–1140.

(24) Pezzella, A.; Panzella, L.; Crescenzi, O.; Napolitano, A.; Navaratnam, S.; Edge, R.; Land, E. J.; Barone, V.; D'Ischia, M. Lack of Visible Chromophore Development in the Pulse Radiolysis Oxidation of 5,6-Dihydroxyindole-2-Carboxylic Acid Oligomers: DFT Investigation and Implications for Eumelanin Absorption Properties. *J. Org. Chem.* **2009**, *74* (10), 3727–3734.

(25) Noriega, R.; Rivnay, J.; Vandewal, K.; Koch, F. P. V.; Stingelin, N.; Smith, P.; Toney, M. F.; Salleo, A. A General Relationship between Disorder, Aggregation and Charge Transport in Conjugated Polymers. *Nat. Mater.* **2013**, *12* (11), 1038–1044.

(26) Fornari, R. P.; Blom, P. W. M.; Troisi, A. How Many Parameters Actually Affect the Mobility of Conjugated Polymers? *Phys. Rev. Lett.* **2017**, *118* (8), 086601.

(27) Pezzella, A.; Vogna, D.; Prota, G. Atropoisomeric Melanin Intermediates by Oxidation of the Melanogenic Precursor 5,6-Dihydroxyindole-2-Carboxylic Acid under Biomimetic Conditions. *Tetrahedron* **2002**, *58* (19), 3681–3687.

(28) Pezzella, A.; Napolitano, A.; D'Ischia, M.; Prota, G.; Seraglia, R.; Traldi, P. Identification of Partially Degraded Oligomers of 5,6-Dihydroxyindole-2-Carboxylic Acid in Sepia Melanin by Matrix-Assisted Laser Desorption/Ionization Mass Spectrometry. *Rapid Commun. Mass Spectrom.* **1997**, *11*, 368.

(29) Pezzella, A.; Iadonisi, A.; Valerio, S.; Panzella, L.; Napolitano, A.; Adinolfi, M.; D'Ischia, M. Disentangling Eumelanin “Black Chromophore”: Visible Absorption Changes as Signatures of Oxidation State- and Aggregation-Dependent Dynamic Interactions in a Model Water-Soluble 5,6-Dihydroxyindole Polymer. *J. Am. Chem. Soc.* **2009**, *131*, 15270.

(30) Pezzella, A.; Panzella, L.; Crescenzi, O.; Napolitano, A.; Navaratnam, S.; Edge, R.; Land, E. J.; Barone, V.; D'Ischia, M. Short-Lived Quinonoid Species from 5,6-Dihydroxyindole Dimers En Route to Eumelanin Polymers: Integrated Chemical, Pulse Radiolytic, and Quantum Mechanical Investigation. *J. Am. Chem. Soc.* **2006**, *128* (48), 15490–15498.

(31) Ascione, L.; Pezzella, A.; Ambrogi, V.; Carfagna, C.; D'Ischia, M. Intermolecular  $\pi$ -Electron Perturbations Generate Extrinsic Visible Contributions to Eumelanin Black Chromophore in Model Polymers with Interrupted Interring Conjugation. *Photochem. Photobiol.* **2013**, *89* (2), 314–318.

(32) Panzella, L.; Gentile, G.; D'Errico, G.; Della Vecchia, N. F.; Errico, M. E.; Napolitano, A.; Carfagna, C.; D'Ischia, M. Atypical Structural and  $\pi$ -Electron Features of a Melanin Polymer That Lead to Superior Free-Radical-Scavenging Properties. *Angew. Chem., Int. Ed.* **2013**, *52* (48), 12684–12687.

(33) Micillo, R.; Panzella, L.; Koike, K.; Monfrecola, G.; Napolitano, A.; D'Ischia, M. “Fifty Shades” of Black and Red or How Carboxyl Groups Fine Tune Eumelanin and Pheomelanin Properties. *Int. J. Mol. Sci.* **2016**, *17*, 746.

(34) Zhang, Y.; Liu, C.; Balaeff, A.; Skourtis, S. S.; Beratan, D. N. Biological Charge Transfer via Flickering Resonance. *Proc. Natl. Acad. Sci. U. S. A.* **2014**, *111*, 10049.

(35) Jackson, N. E.; Kohlstedt, K. L.; Savoie, B. M.; Olvera de la Cruz, M.; Schatz, G. C.; Chen, L. X.; Ratner, M. A. Conformational Order in Aggregates of Conjugated Polymers. *J. Am. Chem. Soc.* **2015**, *137* (19), 6254–6262.

(36) Wang, S.; Fazzi, D.; Puttisong, Y.; Jafari, M. J.; Chen, Z.; Ederth, T.; Andreassen, J. W.; Chen, W. M.; Facchetti, A.; Fabiano, S. Effect of Backbone Regiochemistry on Conductivity, Charge Density, and Polaron Structure of n-Doped Donor-Acceptor Polymers. *Chem. Mater.* **2019**, *31*, 3395.

(37) Qin, T.; Troisi, A. Relation between Structure and Electronic Properties of Amorphous MEH-PPV Polymers. *J. Am. Chem. Soc.* **2013**, *135*, 11247.

(38) Frisch, M. J.; Trucks, G. W.; Schlegel, H. B.; Scuseria, G. E.; Robb, M. A.; Cheeseman, J. R.; Scalmani, G.; Barone, V.; Mennucci, B.; Petersson, G. A.; et al.: *Gaussian16*, Revision C.01; Gaussian Inc.: Wallingford, CT, 2016.

(39) O'Boyle, N. M.; Tenderholt, A. L.; Langner, K. M. Cclib: A Library for Package-Independent Computational Chemistry Algorithms. *J. Comput. Chem.* **2008**, *29*, 839.